Simulation Research On Space-ranging Vector Guidance System Of Tubular Magnetic Sources

Xinyu Dou

Intelligence and Information Engineering College, Tangshan University

Corresponding author. E-mail: douxinyu2007@163.com

Received: Apr. 21, 2024; Accepted: Jul. 25, 2024

There is a huge gap between domestic and foreign technology in measurement while drilling (MWD) field, especially in the aspect of MWD of magnetic properties; domestic technology is still lacking in systematic research. Taking the measurement of the magnetic properties of bottom hole assembly (BHA) as the main line, on the one hand, the magnetic field distribution law of built-in BHA magnetic sub in rock stratum is studied; on the other hand, the theoretical research and preliminary design of the magnetic field vector measurement guidance system are carried out for monitoring the space distance between the drilling well and drilled well. Firstly, the three-dimensional space magnetic field law model of tubular magnetic sub of BHA is established by applying the basic theory of the spatial magnetic field law of permanent magnets, and on the basis of this model, the calculation formula of the three-dimensional space magnetic field law of tubular magnetic sub is deduced. Secondly, the magnetic field law of tubular magnetic sub in rock stratum is studied by using the derived formula, and the calculation rules are summarized by combining graphic calculation and numerical calculation. Finally, the calculation rules are applied to calculate separately the adjacent wells distance of the coalbed methane (CBM) connected well and heavy oil double horizontal well, the core algorithm of the magnetic field vector measurement guidance system is obtained, and the calculation rules of the vector distance are verified and analyzed. This method can avoid the complex calculation of permeability and accurately calculate the vector distance between adjacent wells. Meanwhile, this method can be used to guide the research of tubular magnetic sub, magnetic field measurement systems, and the operation of measurement tools.

Keywords: three-dimensional magnetic field mode; magnetic field intensity; tubular magnet; vector distance; calculation formulas

http://dx.doi.org/10.6180/jase.202506_28(6).0011

1. Introduction

In order to meet the increasing requirements of oil and gas exploration and development, the major drilling service companies in the world have developed various downhole measurement while drilling systems [1]. However, compared with the international advanced level, there is still a big gap in the research field in China, especially in the dynamic characteristics of BHA and magnetic characteristics (that is, the magnetic field intensity of the magnetic sub in the rock formation space point in the BHA) while drilling is still lack of systematic research [2].

Research indicates that the development of heavy oil using double horizontal well technology and the development of coalbed methane (CBM) using multi-branched well technology [3] have achieved the desired results, and the guidance system must be applied to drill this kind of special well. Guidance equipment that uses the measurement of three-dimensional magnetic field vectors of electromagnetic field/magnetic field source to judge the space

distance between the measuring point and the emission source has been widely used abroad. In the development of CBM multilateral wells, the devices mentioned above have been rented at a high cost [4, 5], and the construction of multiple connected wells has been completed with remarkable results. Firstly, the magnetic field vector guidance system is discussed, and the tubular magnet space magnetic field distribution formula is derived. Secondly, the magnetic sub space magnetic field distribution law is analyzed by the software; and then the calculation method of the vector distance between the adjacent wells is studied by using the analysis conclusion combined with the model diagram. Finally, the core algorithm of the magnetic field vector guidance system is obtained.

2. Electromagnetic field / magnetic field vector guidance system

2.1. Electromagnetic vector guidance system for crossing rivers and tunnels, etc.

When wells cross rivers and tunnels, the position of the drill bit should be constantly detected to meet the design requirements. An electromagnetic guidance system developed abroad [6, 7] can be used to monitor the direction of this bit. Its hardware system consists of the transmitter and receiver components. The basic structure of the transmitter component is the spiral tube [8, 9].

The electromagnetic field generated by the spiral tube is telemetered by MWD and transmitted to the computer on the well. The vector distance between the electromagnetic transmitter and the receiver is obtained by using the model and software to achieve the purpose of monitoring the borehole trajectory parameters. Because the accuracy requirements of the underground environment for crossing rivers and tunnels are low, spiral tube launching equipment can be applied to such wells. The advantage of this method is that it can realize the measurement while drilling, but the disadvantage is that the measurement distance is limited due to the limitation of the magnetic field intensity of the excitation signal source.

2.2. Electromagnetic vector guidance system for drilling joint butt wells and parallel horizontal wells

In the multi-branch well developed system of the CBM, vertical wells should be drilled around and connected with the main well, and then the vertical well should be used for drainage and gas recovery [10, 11]. This kind of U-shaped connected well requires special tools to achieve. During real-time drilling, a special tubular magnetic sub that should be similar to the shape of the drill collar is attached to the drill bit [12, 13]. The intensity of the exciting magnetic field generated by the magnetic sub can be detected up to 60m from the magnetic source space [14, 15]. A measurement system connected to the cable is placed in the target well to measure the magnitude and direction of the excitation magnetic field. According to the calculation rule, the vector distance between the magnetic sub and the magnetic measurement system is calculated by using the measured magnetic field vector, in order to achieve control of communication between adjacent wells.

Achieving this technology requires a guidance system to monitor the distance of double parallel horizontal wells during drilling. The high-intensity magnetic sub is fixed at the end of the drill bit, and the measuring equipment is lowered into the other corresponding drilled horizontal well by pumping or other methods. During drilling, the direction of drill bit movement is continuously monitored by the guidance system to maintain horizontal and vertical spacing between double horizontal wells [16, 17]. The advantage of this method is that it can improve the detection accuracy, but the disadvantage is that it affects the normal production of the drilled well.

2.3. Electromagnetic vector guidance system for drilling relief wells

To accurately locate the accident well during the drilling of the relief well, the basic principle of the guidance system used in the drilling is as follows. Firstly, the electrode is lowered to the bottom of the relief well through the cable. Secondly, an alternating current with high amplitude and low frequency is injected into the cable, and then an alternating electromagnetic field is generated around the cable and transmitted through the rock space. Thirdly, the pipe string of the accident well inducts the sympathetic current generated by the alternating electromagnetic field from the relief well and excites a new electromagnetic field. Fourthly, the new electromagnetic field returns to the relief well through the rock formation. Finally, the relief well sensor detects the amplitude and direction of the returned electromagnetic field from the accident well; the corresponding distance and orientation are obtained by the calculation model and software in the ground microcomputer. It has been shown to be an accurate tool for locating the position of the pipe string in the accident well, and the application range of positioning is up to 60 m in engineering practice [18, 19]. The advantage of this method is to improve the detection distance, but the disadvantage is that the detection accuracy is not high due to high temperature and high pressure [20–22].

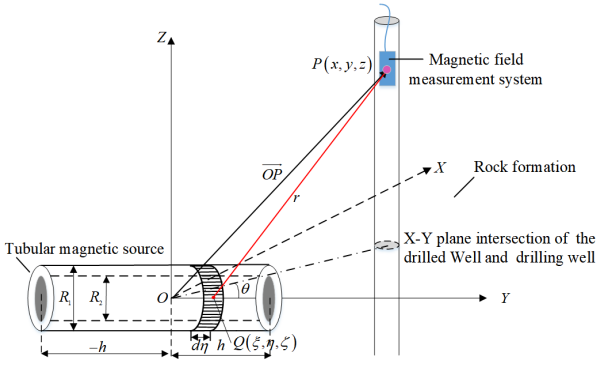

Fig. 1. The model of magnetic field-space of tubular magnet in rock formation

3. Three-dimensional magnetic field law of tubular magnet

During drilling, the complex downhole environment requires higher requirements for the various strengths of the near-bit drilling tools, which leads to the fact that the magnetic sub can only adopt a simple structure similar to the tubular sub of the drill collar. Using the general integral expression method, the expressions of the magnetic field components of arbitrary shape magnet under uniform magnetization are obtained as follows [14]. The model of magnetic field-space of tubular magnet in rock strata is shown in Fig. 1.

$$\begin{cases} B_{ax}=\frac{\mu_0}{4\pi}\left[M_x\int_L ds\int_{-h}^{h}\frac{2x^2-z^2-(y-\eta)^2}{\left[x^2+(y-\eta)^2+z^2\right]^{\frac{5}{2}}}d\eta+M_y\int_L ds\int_{-h}^{h}\frac{3x(y-\eta)}{\left[x^2+(y-\eta)^2+z^2\right]^{\frac{5}{2}}}d\eta+M_z\int_L ds\int_{-h}^{h}\frac{3xz}{\left[x^2+(y-\eta)^2+z^2\right]^{\frac{5}{2}}}d\eta\right] \\ B_{ay}=\frac{\mu_0}{4\pi}\left[M_x\int_L ds\int_{-h}^{h}\frac{3x(y-\eta)}{\left[x^2+(y-\eta)^2+z^2\right]^{\frac{5}{2}}}d\eta+M_y\int_L ds\int_{-h}^{h}\frac{2(y-\eta)^2-x^2-z^2}{\left[x^2+(y-\eta)^2+z^2\right]^{\frac{5}{2}}}d\eta+M_z\int_L ds\int_{-h}^{h}\frac{3z(y-\eta)}{\left[x^2+(y-\eta)^2+z^2\right]^{\frac{5}{2}}}d\eta\right] \\ B_{az}=\frac{\mu_0}{4\pi}\left[M_x\int_L ds\int_{-h}^{h}\frac{3zx}{\left[x^2+(y-\eta)^2+z^2\right]^{\frac{5}{2}}}d\eta+M_y\int_L ds\int_{-h}^{h}\frac{3z(y-\eta)}{\left[x^2+(y-\eta)^2+z^2\right]^{\frac{5}{2}}}d\eta+M_z\int_L ds\int_{-h}^{h}\frac{\left[2z^2-x^2-(y-\eta)^2\right]}{\left[x^2+(y-\eta)^2+z^2\right]^{\frac{5}{2}}}d\eta\right] \end{cases} \tag{1}$$

$$\begin{cases} M_x=\frac{m_x}{S} \\ M_y=\frac{m_y}{S} \\ M_z=\frac{m_z}{S} \end{cases} \tag{2}$$

Where: h is half of the length of the tubular magnetic source, m. B_{ax}, B_{ay}, and B_{az} are three mutually perpendicular components of the space magnetic field outside the pipe string at the measurement point $\mathrm{P}(x,y,z)$, respectively, T; r is the distance between the micro-element point of any section of the magnet and the space point P, m; M_x, M_y, and M_z are the magnet magnetization components in the X, Y, and Z directions, respectively. ξ,η and ζ are the coordinates of the magnetic micro-element on the X, Y, and Z axes, respectively, m; μ_0 is the magnetic permeability of the magnetic field in the rock formation; V is the magnet volume variable, m^3. Eq. (3) can be derived from Eqs. (1) and (2).

$$\begin{cases} B_{ax}=\frac{\mu_0 x}{4\pi}\left\{\frac{m_x z}{c^2}\left[\frac{-d\left[3c+2d^2\right]}{a^{\frac{5}{2}}}-\frac{e\left[3c+2e^2\right]}{b^{\frac{5}{2}}}\right]+m_y\left[\frac{1}{a^{\frac{3}{2}}}-\frac{1}{b^{\frac{3}{2}}}\right]-\frac{m_z z}{c}\left[\frac{d\left[3c+2d^2\right]}{a^{\frac{5}{2}}}-\frac{e\left[3c+2e^2\right]}{b^{\frac{5}{2}}}\right]\right\} \\ B_{ay}=\frac{\mu_0}{4\pi}\left\{m_x x\left[\frac{1}{a^{\frac{3}{2}}}-\frac{1}{b^{\frac{3}{2}}}\right]+m_y\left[\frac{d}{a^{\frac{3}{2}}}-\frac{e}{b^{\frac{3}{2}}}\right]+m_z z\left[\frac{1}{a^{\frac{3}{2}}}-\frac{1}{b^{\frac{3}{2}}}\right]\right\} \\ B_{az}=\frac{\mu_0}{4\pi}\left\{\frac{-m_x xz}{c}\left[\frac{d\left[3c+2d^2\right]}{a^{\frac{5}{2}}}-\frac{e\left[3c+2e^2\right]}{b^{\frac{5}{2}}}\right]+m_y z\left[\frac{1}{a^{\frac{3}{2}}}-\frac{1}{b^{\frac{3}{2}}}\right]+\frac{m_z}{c^2}\left[\frac{d\left[d^2f-(2z^2-x^2)c\right]}{a^{\frac{5}{2}}}-\frac{e\left[e^2f-(2z^2-x^2)c\right]}{b^{\frac{5}{2}}}\right]\right\} \\ a=x^2+(y-h)^2+z^2 \\ b=x^2+(y+h)^2+z^2 \\ c=x^2+z^2 \\ d=y-h \\ e=y+h \\ f=x^2-z^2 \end{cases} \tag{3}$$

When the magnetization direction is along the axial direction of the pipe string, that is, along the Y-axis direction in Fig.1, the above formula is simplified as follows.

$$\begin{cases} B_{ax}=\frac{\mu_0}{4\pi}m_y x\left\{\frac{1}{\left[x^2+z^2+(y-h)^2\right]^{\frac{3}{2}}}-\frac{1}{\left[x^2+z^2+(y+h)^2\right]^{\frac{3}{2}}}\right\} \\ B_{ay}=\frac{\mu_0}{4\pi}m_y\left\{\frac{y-h}{\left[x^2+z^2+(y-h)^2\right]^{\frac{3}{2}}}-\frac{y+h}{\left[x^2+z^2+(y+h)^2\right]^{\frac{3}{2}}}\right\} \\ B_{az}=\frac{\mu_0}{4\pi}m_y z\left\{\frac{1}{\left[x^2+z^2+(y-h)^2\right]^{\frac{3}{2}}}-\frac{1}{\left[x^2+z^2+(y+h)^2\right]^{\frac{3}{2}}}\right\} \end{cases} \tag{4}$$

The above is the whole process of deducing the spatial magnetic field law of a tubular magnet. Eq. (4) is the three-component law formula for the magnetic field intensity of the any point in space, it also concerns the distribution law of the magnetic field space of the tubular magnet [22, 23].

Substitute $k=\mu_0 m_y/4\pi$ in Eq. (4), then Eq. (4) can be simplified to Eqs. (5) to (7).

$$B_{ax}=kx\left\{\frac{1}{\left[x^2+z^2+(y-h)^2\right]^{\frac{3}{2}}}-\frac{1}{\left[x^2+z^2+(y+h)^2\right]^{\frac{3}{2}}}\right\} \tag{5}$$

$$B_{ay}=k\left\{\frac{y-h}{\left[x^2+z^2+(y-h)^2\right]^{\frac{3}{2}}}-\frac{y+h}{\left[x^2+z^2+(y+h)^2\right]^{\frac{3}{2}}}\right\} \tag{6}$$

$$B_{az}=kz\left\{\frac{1}{\left[x^2+z^2+(y-h)^2\right]^{\frac{3}{2}}}-\frac{1}{\left[x^2+z^2+(y+h)^2\right]^{\frac{3}{2}}}\right\} \tag{7}$$

The vector distance cannot be calculated directly from the above formulas. In this paper, the combination of formula derivation and Matlab software is used to simulate and analyze the regular variation pattern of each component of the magnetic field with each variable according to the above formula [23], in order to find the rule for the calculation of the vector distance.

3.1. Component B_{ax} variation rule with variable

3.1.1. B_{ax} variation rule with variable x

Eq. (8) is derived by taking the partial derivative to x in Eq. (5).

$$f'_{ax}(x)=k\left\{\begin{array}{l}\dfrac{1}{\left[x^2+z^2+(y-h)^2\right]^{\frac{3}{2}}}-\dfrac{1}{\left[x^2+z^2+(y+h)^2\right]^{\frac{3}{2}}}\\ -\dfrac{3x^2}{\left[x^2+z^2+(y-h)^2\right]^{\frac{5}{2}}}+\dfrac{3x^2}{\left[x^2+z^2+(y+h)^2\right]^{\frac{5}{2}}}\end{array}\right\} \tag{8}$$

In order to find the extreme value of Eq. (8), Eq. (9) is obtained by making Eq. (8) equal to 0.

$$f'_{ax}(x)=0 \tag{9}$$

The solution of Eq. (9) is Expression Eq. (10).

$$x=\pm\frac{\sqrt{z^2+(y\pm h)^2}}{2} \tag{10}$$

Based on the calculations and analysis above, the following conclusions can be drawn:

1. The maximum coordinate value of each change curve is $\left(\pm\sqrt{z^2+(y\pm h)^2}/2, B_{\text{amm}}\right)$. The application of this correspondence law in practice will be analyzed in detail later.
2. The B_{ax} change with the variable x is related to $\pm\sqrt{z^2+(y\pm h)^2}/2$, that is, the variable y remains unchanged, and the curve change law of the B_{ax} component with x remains unchanged when z takes a different fixed value, but the position of the maximum value increases as z increases; the variable z remains unchanged, and the curve of the B_{ax} component with x also remains unchanged when y takes different fixed values, but the position where the maximum value appears increases with increasing variable y.

3.1.2. B_{ax} variation rule with variable y

Eq. (11) is derived by taking the partial derivative with respect to y in Eq. (5).

$$f_{ax}(y)=3kx\left\{\frac{-(y-h)}{\left[x^2+z^2+(y-h)^2\right]^{\frac{5}{2}}}+\frac{(y+h)}{\left[x^2+z^2+(y+h)^2\right]^{\frac{5}{2}}}\right\} \tag{11}$$

To find the extreme value of Eq. (11), Eq. (12) is obtained by making Eq. (11) equal to 0.

$$f'_{a\alpha}(y)=0 \tag{12}$$

Since Expression Eq. (12) cannot be solved directly, Expression Eq. (13) is obtained by fitting Matlab software fitting.

$$y=\pm\frac{\sqrt{x^2+z^2}}{2} \tag{13}$$

According to calculations and analysis, the following conclusions can be drawn:

1. The maximum value coordinate of each change curve is $\left(\pm\sqrt{x^2+z^2}/2, B_{\text{avn}}\right)$. The application of the corresponding law in practice will be analyzed in detail later.
2. The change in B_{ax} with the variable y is related to $\pm\sqrt{x^2+z^2}/2$; that is, the variable x remains unchanged; when z takes the different fixed values, the curve change law of the component B_{ax} with y remains unchanged, but the position where the maximum value increases with increasing z; variable z remains unchanged, and the curve change law of the component B_{ax} with y also remains unchanged when x takes different fixed values, but the maximum value position increases with increasing x.

3.1.3. B_{ax} variation rule with variable z

Eq. (14) is derived by taking the partial derivative with respect to z in Eq. (5).

$$f'_{ax}(z) = -3kxz\left\{\frac{1}{\left[x^2+z^2+(y-h)^2\right]^{\frac{5}{2}}} - \frac{1}{\left[x^2+z^2+(y+h)^2\right]^{\frac{5}{2}}}\right\} \tag{14}$$

Similarly, make Eq. (14) equal to 0 to obtain the corresponding extreme value.

$$f'_{ax}(z) = 0 \tag{15}$$

The solution of Eq. (15) is Expression Eq. (16).

$$z = 0 \tag{16}$$

Based on the calculations and analysis above, the following conclusions can be drawn:

1. The maximum coordinate value of each change curve corresponds to $(0, B_{\text{axm}})$, and the application of this corresponding law in practice will be analyzed in detail later.

2. As the variable x takes different fixed values, the curve change law of the B_{ax} component with z remains unchanged, and the Z-axis coordinate position corresponding to the maximum magnetic field intensity unchanges with the variable x. As the variable y takes different fixed values, the curve change law of the component B_{ax} with y also remains unchanged, and the Z-axis coordinate position corresponding to the maximum magnetic field intensity unchanges with the variable y.

3.2. Component B_{ay} variation rule with variable

3.2.1. B_{ay} variation rule with variable x

Similarly, construct the following function, as shown in Eq. (17).

$$f'_{ay}(x) = -3kx\left\{\frac{1}{\left[x^2+z^2+(y-h)^2\right]^{\frac{5}{2}}} - \frac{1}{\left[x^2+z^2+(y+h)^2\right]^{\frac{5}{2}}}\right\} = 0 \tag{17}$$

The extreme value of B_{ay} is calculated to occur when x is equal to 0(x=0).

3.2.2. B_{ay} variation rule with variable y

Construct the following function, as shown in Eq. (18).

$$f'_{ay}(y) = k\left\{\frac{x^2+z^2-2(y-h)^2}{\left[x^2+z^2+(y-h)^2\right]^{\frac{5}{2}}} - \frac{x^2+z^2-2(y+h)^2}{\left[x^2+z^2+(y+h)^2\right]^{\frac{5}{2}}}\right\} = 0 \tag{18}$$

It is calculated that B_{ay} has an extreme value when y is equal to 0(y=0).

3.2.3. B_{ay} variation rule with variable z

Construct the following function, as shown in Eq. (19).

$$f'_{ay}(z) = -3kz\left\{\frac{1}{\left[x^2+z^2+(y-h)^2\right]^{\frac{5}{2}}} - \frac{1}{\left[x^2+z^2+(y+h)^2\right]^{\frac{5}{2}}}\right\} = 0 \tag{19}$$

It is calculated that B_{ay} has an extreme value when z is set to 0 (z=0). Analysis of the above calculations indicates that:

1. The Bay component presents different extreme value directions with the change of different variables. The component B_{ay} takes the maximum positive value when x is equal to 0 , and gradually decreases with increasing positive (negative) directions x; B_{ay} takes the maximum negative value when y is set to 0 , and $|B_{ay}|$ gradually decreases with increasing positive (negative) directions y; B_{ay} takes the maximum value when z is equal to 0 , and $|B_{ay}|$ gradually decreases with increasing positive (negative) directions z.

2. Although the direction of the maximum value Bay varies with the changing of different variables, it can be concluded that the maximum value is obtained at $(0, B_{\text{avm}})$, and the apparent maximum value is only obtained at this point. The rule will be applied to the distance calculation below.

3.3. Component Baz variation rule with variable

The variation law of B_{ax} and B_{az} magnetic fields is similar, so the rule diagram of component B_{az} is similar to the variation law of B_{ax}, which will not be be described in detail here.

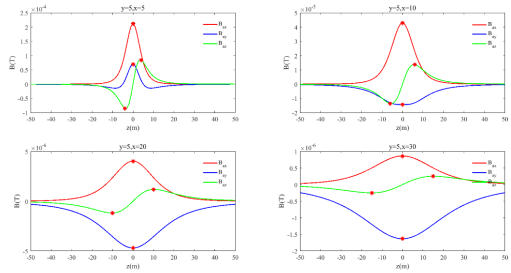

Fig. 2. The graph of the variation law of B_{ax}, B_{ay}, and B_{az} with z under the conditions of $y = 5, k = 0.1, h = 0.25$, and x takes different values.

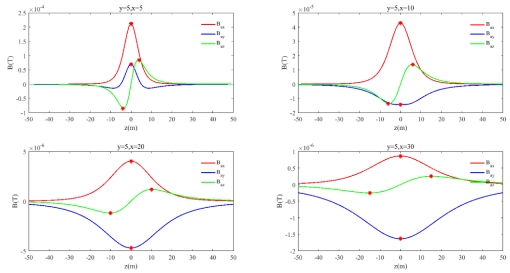

Fig. 3. The graph of the variation law of B_{ax}, B_{ay}, and B_{az} with z under the conditions of $x = 5, k = 0.1, h = 0.25$ and y takes different values.

4. Analysis and application of the overall variation law of the three-component magnetic field intensity to calculate the distance between the connected wells

4.1. The variation law with the variable z and the calculation of the distance between the connected wells

Through the analysis and calculation above, it can be seen that when there is only the maximum value in the B_{ax} and B_{ay} graphs and curves, the corresponding coordinate is $(0, B_{am})$; when there is a maximum (minimum) value in the B_{az} graphs and curves, the corresponding coordinate is $\left(\pm\sqrt{z^2 + (y \pm h)^2}/2, B_{acm}\right)$

The variation law of the components B_{ax}, B_{az}, and B_{ay} with z is simulated by the software in this party, and the variation law of each magnetic field component with the Z-axis coordinate in Fig. 1 is discussed. When $y = 5, k = 0.1, h = 0.25$, and x are taken as 5, 10, 20, and 30 respectively, the curve of magnetic field strength changes with variable z is shown in Fig. 2. When $x = 5, k = 0.1, h = 0.25$, and y are taken as 5, 10, 20, and 30 respectively, the curve of magnetic field strength changes with variable z is shown in Fig. 3. The curves are represented by 3 colors, where red curve represents the B_{ax} component, the green curve represents the B_{az} component, and the blue curve represents the B_{ay} component.

According to the rule of change of B_{ax}, B_{az}, and B_{ay} with z in Figs. 2 and 3 above, the following conclusions can be drawn.

1. The figure '*' in each component can correspond well to the extreme value of the graph; that is, when there is only the maximum value in the curves of the B_{ax} and B_{ay} graph, the maximum value that corresponds to the coordinate is $(0, B_{am})$. When there are maximum and minimum values in the B_{az} graph curve, the value in the graph also corresponds well with the coordinates $\left(\pm\sqrt{z^2 + (y \pm h)^2}/2, B_{can}\right)$. In other words, as x and y take different fixed values, the component B_{ax} and B_{ay} takes the maximum value (or the negative maximum value). when the variable z is equal to 0 . When B_{az} takes the maximum or minimum value, the variable z is shown in Eq. (20).

$$z = \pm\frac{\sqrt{x^2 + (y \pm h)^2}}{2} \tag{20}$$

2. It can be seen from that when the variable z changes within $0 \sim 50$ m (the fixed values of x and y should also be within 50 m), there will always be an intersection point between the components B_{ax} and B_{az}, which exactly verifies the relationship between Eqs. (5) and (7), that is, B_{ax} and B_{az} are also equal in size when the variable values are equal.

3. Along the Z-axis direction, the B_{az} component always obtains the maximum and minimum values, while the ingredients B_{ax} and B_{ay} always get the only maximum value or the maximum negative value. Furthermore, the three parts get extreme points according to the law of conclusion (1), which can be used to calculate the vector distance in the U-shaped butt joint wells.

4.2. Calculation distance in connected wells

According to the conclusions that the magnetic field intensity components B_{ax}, B_{az}, and B_{ay} vary with z and the measurement equipment used in the actual measurement, the expression model of the measurement process and calculation of the vector distance in the connected well is established in Fig. 4.

As shown in Fig. 4, R is in the plane formed by XOY, which represents the spatial distance between the magnetic source and the midpoint of the AB , its size $|R| = \sqrt{x_P^2 + y_P^2}$, and the angle included with the Y-axis is α, $\tan\alpha = x/y$. The magnetic field measurement system is

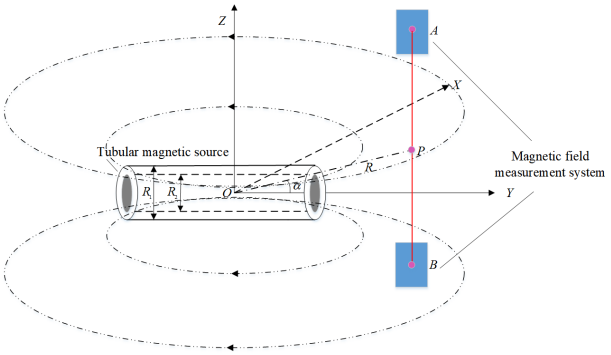

Fig. 4. Schematic diagram of the vector distance in connected wells

used to run into the bottom of the well that has been drilled along the positive Z-axis. When the three components of the magnetic field intensity are measured, the measurement data are transmitted to the processing system on the ground through the cable.

The point A (x_A, y_A, z_A) represents the spatial point where the measurement system obtains where the measurement system obtains the minimum value of the B_{az} component. The point P represents the midpoint of AB , and the maximum point of components B_{ax} and B_{ay} (it can be seen that the midpoint of AB coincides with the maximum point of components B_{ax} and B_{ay}), and its coordinate is set to P $(x_P, y_P, 0)$.

B_{ax} and B_{az} always intersect during the measurement process, and its coordinate is C $(x_C \ \ y_C, z_C)$. Since $x_C = z_C$ exists, the coordinate of point C is (z_C, y_C, z_C).

Combining Figs. 2 and 3, it can be shown that when the measurement system moves along the Z-axis, the components B_{az} will obtain maximum and minimum values, respectively. Record the coordinates of the two extreme points when the component B_{az} measured by the measuring system during the movement is at the maximum value and the minimum value, respectively, and the distance between the two extreme points is |AB|.

The vector distance and direction angle are obtained by comprehensive analysis.

1. According to Eq. (20), it can be derived from Formula Eq. (21).

$$|AB| = |OP| = |R| = \sqrt{x_P^2 + y_P^2} = |z_A - z_B| \quad (21)$$

Therefore, the magnitude of the vector $\overrightarrow{OP}$ in Fig. 3 can be obtained by recording the coordinate values of the maximum points A and B in Fig. 3 in each measurement [22, 23].

2. The four points A, B, P, and the intersection point C are the position points obtained by analyzing the components during the measurement process of the measurement system, and the measurement equipment moves downward along the Z-axis direction, then:

$$x_A = x_B = x_P = x_C = z_C \quad (22)$$

$$y_A = y_B = y_P = y_C \quad (23)$$

Combining the above formula, it can get Eqs. (24) and (25).

$$y_P = \sqrt{|R|^2 - z_C^2} \quad (24)$$

$$\tan\alpha = \frac{x_P}{y_P} = \frac{z_C}{\sqrt{|R|^2 - z_C^2}} \quad (25)$$

Thus, the direction angle of the vector $\overrightarrow{OP}$ is determined in the space coordinate system of the magnetic sub in Fig. 1 is determined. According to the calculation methods of conclusions (1) and (2), it is not necessary to involve the magnetic field permeability in the formation of the rock to calculate the vector and avoid the problem that the imprecision of magnetic permeability affects the accuracy of the calculation results. Therefore, combining the above methods can accurately determine the vector $\overrightarrow{OP}$ to be calculated and controlled in the connected wells.

5. analysis and application of the overall variation law of the three-component magnetic field intensity to calculate the parallel double horizontal well distance

5.1. Variation of the magnetic field component with variable y and calculation distance in parallel double horizontal wells

This part simulates the variation law of the elements B_{ax}, B_{az}, and B_{ay} with y through software, and discusses the variation relationship of each magnetic field component with the variable y in Fig. 1 of the model. When $x = 5, k = 0.1, h = 0.25$, and z are taken as 5, 10, 20, and 30 respectively, the curve of magnetic field strength changes with variable y is shown in Fig. 5. When $z = 5, k = 0.1, h = 0.25$, and x are taken as 5, 10, 20, and 30 respectively, the curve of magnetic field strength changes with variable y is shown in Fig. 6.

According to the variation law of the elements B_{ax}, B_{az}, and B_{ay} with y in Figs. 5 and 6 above, the following conclusions can be drawn.

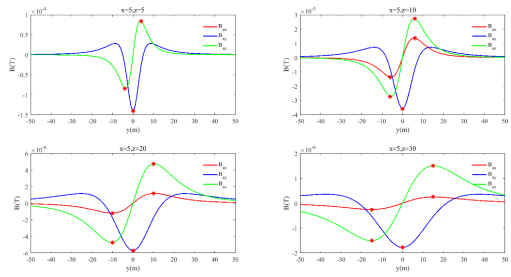

Fig. 5. The graph of the variation law of B_{ax}, B_{ay}, and B_{az} with y under the conditions of $x = 5, k = 0.1, h = 0.25$ and z takes different values.

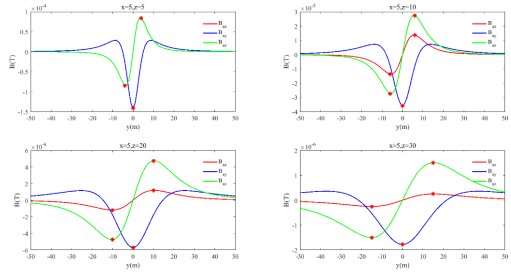

Fig. 6. The graph of the variation law of B_{ax}, B_{ay}, and B_{az} with y under the conditions of $z = 5, k = 0.1, h = 0.25$ and x takes different values.

1. The "*" in each component can correspond to the extreme value of the graph, that is, when there is only the maximum value in the B_{ay} graph, and it corresponds to the coordinate $\left(0, B_{\text{aym}}\right)$; when there can be maximum and minimum values in the B_{ax} and B_{az} graphs, the value in the graph also corresponds to the coordinate point $\left(\pm\sqrt{x^2+z^2}/2, B_{\text{an}}\right)$. The corresponding relationship indicates that x and y take different fixed values, B_{ay} takes the maximum value (or negative maximum value) when the variable z is equal to 0.B_{ax} and B_{az} take the maximum or minimum value when the variable y equals $y = \pm\sqrt{x^2+z^2}/2$.

2. As the variable y changes, the components B_{ax} and B_{az} always maintain a proportional relationship (it is established when the variable y is not 0), and it can be drawn as Eq. (26) Formula (26).

$$\frac{B_{ax}}{B_{\alpha c}} = \frac{x_A}{z_A} = \frac{x_B}{z_B} = \frac{x}{z} \tag{26}$$

Along the Y-axis direction, the components B_{ax} and B_{az} consistently achieve maximum and minimum values, while the components B_{ay} always obtain unique maximum or maximum negative values. Furthermore, the three components obtain extreme values according to the law as in conclusion (1), which can be used to calculate the vector distance in double horizontal wells.

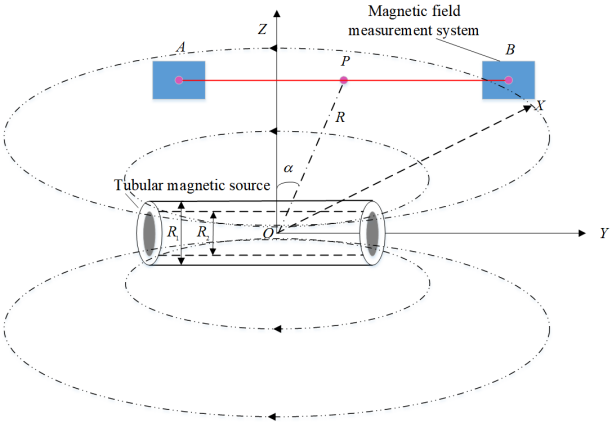

Fig. 7. Schematic diagram of the vector distance representation in double horizontal well.

5.2. Calculation of the intermediate distance in double horizontal wells

According to the conclusion that the magnetic field intensity components B_{ax}, B_{az}, and B_{ay} vary with y and the measurement equipment used in the actual measurement, a representation model for the measurement and calculation of vector distance in double horizontal wells as shown in Fig. 7 Fig. 7 is established.

As shown in Fig. 7, R is in the plane formed by XOZ, which represents the spatial distance between the magnetic source and the midpoint of AB , its size is $|R| = \sqrt{x_P^2 + z_P^2}$, and the angle included with the Z-axis is α. The magnetic field measurement system drives down the drilled bottom hole along the positive Y-axis. When the three components of the magnetic field intensity are measured, the detection data are transmitted via cable to the processing system on the well.

Where $\underline{A}\left(x_A, y_A, z_A\right)$ represents the point when the measurement system obtains the maximum value of the components B_{ax} and B_{az} (it can be seen from Figs. 5 and 6 that when B_{ax} and represents the point at which the measurement system obtains the minimum value of the components B_{ax} and B_{az}. Point P represents the midpoint of AB , and also represents the maximum point of the B_{ay} component, and the coordinate is set to $\left(x_P, 0, z_P\right)$.

Combining Figs. 5 and 6 , it can be indicated that when the measurement system moves along the Y-axis direction, the components B_{az} and B_{ax} will simultaneously achieve the maximum value at the same point and the minimum

value at another same point. When the components B_{az} and B_{ax} measured by the measuring system are at the maximum and minimum values, respectively, the coordinates of the two extreme points are recorded, and the distance between the two extreme points is |AB|.

By comprehensive analysis of Figs.5-6, the magnitude and direction angle of the vector distance can be calculated by Eq. (27) that can be known from Eq. (21).

$$|AB| = |OP| = |R| = \sqrt{x_P^2 + z_P^2} = |y_A - y_B| \tag{27}$$

Therefore, the magnitude of the vector in Fig. 7 can be obtained by recording the coordinates of the most valuable points A and B in Fig. 7 during each measurement.

The three points A, B, and P are the position points obtained by analyzing the components during the measurement process of the measurement system, and the measurement equipment moves along the Y-axis direction, so there is the following relationship.

$$\begin{cases} x_A = x_B = x_P \\ Z_A = z_B = z_P \end{cases} \tag{28}$$

From Equations Eqs. (25), (27) and (28) and $\tan\alpha = x_P/z_P$, Formula Eq. (29) can be deduced as follows.

$$\tan\alpha = \frac{B_{ax}}{B_{\alpha x}} = \frac{B_{a\alpha d}}{B_{a\alpha A}} = \frac{B_{\alpha\beta}}{B_{aB}} \quad \left(\frac{B_{ax}}{B_{\alpha c}} \neq 0\right) \tag{29}$$

Thus, the direction angle of the vector in Fig. 7 is determined. According to the calculation methods of conclusions (1) and (2), it is not necessary to involve the magnetic field permeability in the rock formation in the vector calculation, in order to avoid the inaccuracy of the calculation result caused by the imprecision of the permeability.

Therefore, the vector $\overrightarrow{OP}$ to be calculated and controlled in the connected wells can be accurately determined by combining the above methods. In this paper, the general integral method is used to derive the adjacent well calculation formula, which has the advantages of good generality and high ranging accuracy, and the disadvantages of large calculation amount. In contrast, the literature [24] assumes the magnetic source as a magnetic dipole (ignoring the magnetic source size), and then deduces the adjacent well location formula, which has the advantage of relatively small calculation amount and the disadvantage of too many assumptions, it cannot guarantee the accuracy of distance measurement.

5.3. Calculation of interference magnetic field

To eliminate magnetic interference in double horizontal wells, the particularity of coordinate point $y = 0$ is used to calculate the interference magnetic field in this method. As can be seen from the correlation Eqs. (21), (25), (27) and (29) for calculating the distance of the vector, the calculation process has nothing to do with the intensity component B_{ay} generated by the magnetic sub, but only with the components B_{ax} and B_{az}. Therefore, the magnetic interference discussed only considers the magnetic interference of the two related components.

Suppose that the component of the total magnetic field B_y obtained by the sensor is B_{axx} and B_{azv} when the variable y is 0 . The magnetic interference component is:

$$\begin{cases} B_{gx} = B_{av} - B_{ax} \\ B_{gz} = B_{axv} - B_{ac} \end{cases} \tag{30}$$

It can be seen from the above formula that when the variable y is 0 , the magnetic field components generated by the magnetic sub are $B_{ax} = 0$ and $B_{az} = 0$. Eq. (30) can be rewritten as Eq. (31).

$$\begin{cases} B_{gv} = B_{av} \\ B_{gq} = B_{av} \end{cases} \tag{31}$$

When the variable y is 0, the magnetic field measured by the magnetic probe is the value of the magnetic interference component. Therefore, this method is easy to eliminate magnetic field interference and has high precision.

The methods for eliminating magnetic interference in connected Wells are similar to those described above and will not be described in this paper. Therefore, from the above method of eliminating magnetic field interference, it can be seen that the vector distance calculation method obtained in this paper can easily eliminate various interference magnetic fields in each measurement and has high precision, so that the vector distance value obtained has high precision.

6. Conclusions

The space magnetic field model of the tubular magnetic sub is established, and the core formulas of the space magnetic field intensity distribution law of the tubular type magnetic sub are obtained by using the general integral method, which lays a theoretical foundation for the subsequent structural design and optimization of the magnetic sub. The vector distance calculation method is derived, which can lay the core algorithm foundation for the design of the magnetic field intensity measurement system. The research of all kinds of downhole measuring equipment has always been an important development direction of modern drilling technology. Through the research of magnetic sub analysis and vector distance calculation method in magnetic field measuring system, the basic research of magnetic field vector guiding system is carried out.

1. The electromagnetic field/magnetic field vector guidance system is widely used in heavy oil production, CBM development, high-density anti-collision wells, and relief wells.

2. The basic calculation formulas for the vector distance between the tubular magnetic source and the magnetic measurement system are obtained from the spatial magnetic field law model of the tubular magnet, and the three-dimensional distance is obtained through the calculation software.

3. Through simulation and analysis of the magnetic field law formula of the tubular magnetic sub in the bottom hole, the variation law of the magnetic field components with the variables is discussed. The core algorithm for calculating the magnitude and direction of vector distances in connected wells and double horizontal wells is obtained by using the eigenvalues of the law diagram (including the extreme value, peak value, and intersection value of the magnetic field components) and the measured values of the measuring equipment.

4. This method can avoid the complex calculation of permeability and accurately calculate the vector distance between adjacent wells. Meanwhile, this method can be used to guide the research of tubular magnetic sub, magnetic field measurement systems, and the operation of measurement tools.

The above research results are a pioneering exploration of magnetic field vector guidance technology applied to CBM well connectivity and monitoring of the spacing between two wells when drilling double horizontal wells. Although after more than 10 years of development abroad, it has been mature and applied in the field, but its technology is kept secret in China, there is no relevant literature in China and no relevant research has been carried out. Through theoretical research, this paper lays a foundation for the design of the magnetic sub structure of the guidance system, and obtains the core theory and algorithm of the magnetic field vector guidance technology, completing the basic research of the guidance system.

References

[1] G. Deli and D. Binbin, (2016) *"Development of the magnetic guidance drilling technique in complex well engineering"* **Petroleum drilling techniques *44***(5): 1–9.

[2] X. Dou, H. Liang, and Y. Liu, (2018) *"Anticollision method of active magnetic guidance ranging for cluster wells"* **Mathematical Problems in Engineering *2018***(1): 7583425.

[3] A.-M. Al-Bahlani and T. Babadagli, (2009) *"SAGD laboratory experimental and numerical simulation studies: A review of current status and future issues"* **Journal of Petroleum Science and Engineering *68***(3-4): 135–150.

[4] D. A. Wood, (2015) *"Drilling and borehole techniques relevant to natural gas exploration and development: a collection of published research (2009–2015)"* **Journal of Natural Gas Science and Engineering *26***: 396–408.

[5] B. Diao, D. Gao, and Z. Wu, (2011) *"Magnet ranging calculation method of twin parallel horizontal wells steerable drilling"* **Journal of China university of petroleum *35***(6): 71–75.

[6] B. Diao and D. Gao, (2015) *"A magnet ranging calculation method for steerable drilling in build-up sections of twin parallel horizontal wells"* **Journal of Natural Gas Science and Engineering *27***: 1702–1709.

[7] B. Diao and D. Gao, (2013) *"Study on a ranging system based on dual solenoid assemblies, for determining the relative position of two adjacent wells"* **CMES: Computer Modeling in Engineering & Sciences *90***(1): 77–90.

[8] D. Gao, B. Diao, Z. Wu, and Y. Zhu, (2013) *"Research into magnetic guidance technology for directional drilling in SAGD horizontal wells"* **Petroleum Science *10***: 500–506.

[9] T. Liu and B. Wang, (2011) *"Study of magnetic ranging technology in horizontal directional drilling"* **Sensors and Actuators A: Physical *171***(2): 186–190.

[10] G. Liu, Q. Yang, Z. Dong, B. He, and Z. Geng, (2013) *"A drill bit vibration anti-collision monitoring system and field experiment"* **Natural Gas Industry *33***(6): 66–70.

[11] Z. Guan, Y. Liu, Y. Shi, K. Wei, J. Wang, H. Liang, and H. Zhang, (2010) *"Problems and developing direction of anti-collision technology in the dense well pattern area"* **Procedia Engineering *7***: 304–311.

[12] M. Marchetti, V. Sapia, and A. Settimi, (2013) *"Magnetic anomalies of steel drums: a review of the literature and research results of the INGV"* **Annals of geophysics *56***(1): R0108–R0108.

[13] B. Tu, D. Li, E. Lin, B. Luo, and Y. Wang, (2010) *"Analysis of drilling parallel horizontal twin wells rotating magnetic beacons magnetic field strength size in SAGD"* **Proceedings of the PIERS Proceedings *7***: 5–8.

[14] J. McGeough, M. Leu, K. Rajurkar, A. De Silva, and Q. Liu, (2001) *"Electroforming process and application to micro/macro manufacturing"* **CIRP Annals *50***(2): 499–514.

[15] C. Hu, M. Li, M. Q.-H. Meng, S. Song, et al., (2010) *"A new tracking system for three magnetic objectives"* **IEEE Transactions on Magnetics *46***(12): 4023–4029.

[16] Z. Wu, D. Gao, and B. Diao, (2015) *"An investigation of electromagnetic anti-collision real-time measurement for drilling cluster wells"* **Journal of Natural Gas Science and Engineering *23***: 346–355.

[17] S. Feng, D. Liu, X. Cheng, H. Fang, and C. Li, (2017) *"A new segmentation strategy for processing magnetic anomaly detection data of shallow depth ferromagnetic pipeline"* **Journal of Applied Geophysics *139***: 65–72.

[18] C. C. Finlay, S. Maus, C. Beggan, T. Bondar, A. Chambodut, T. Chernova, A. Chulliat, V. Golovkov, B. Hamilton, M. Hamoudi, et al., (2010) *"International geomagnetic reference field: the eleventh generation"* **Geophysical Journal International *183***(3): 1216–1230.

[19] S. D. Billings, C. Pasion, S. Walker, and L. Beran, (2006) *"Magnetic models of unexploded ordnance"* **IEEE Transactions on Geoscience and Remote sensing *44***(8): 2115–2124.

[20] P. Liexin, S. Yinao, S. Limin, et al., (2010) *"Research on self-adapting allocation technique based on the electromagnetic drilling while measurement system"* **Drilling Production Technology *33***(4): 1–4.

[21] S. Chun, F. Xinxin, C. Zhiwei, et al., (2017) *"ANSYS analysis of effects of strata beddings on EM-MWD signal transmission"* **Drilling & Production Technology *40***(4): 7–9.

[22] X. Yan, H. Liang, X. Dou, M. Qing, and X. Cao, (2022) *"An active magnetic ranging method for drilling cluster wells based on casing current excitation"* **Journal of Petroleum Science and Engineering *208***: 109784.

[23] L. Ren, H. Jiang, J. Zhao, R. Lin, Z. Wang, and Y. Xu, (2022) *"Theoretical study on fracture initiation in deep perforated wells with considering wellbore deformation"* **Journal of Petroleum Science and Engineering *211***: 110141.

[24] D. X.Y., L. H.Q., and S. W., (2016) *"Double horizontal electromagnetic radial distance calculation method study"* **Science Technology and Engineering *16***(33): 24–28.